Hindawi Publishing Corporation
EURASIP Journal on Wireless Communications and Networking
Volume 2006, Article ID 16281, Pages 1–8
DOI 10.1155/WCN/2006/16281

Space-Time Water-Filling for Composite MIMO Fading Channels

Zukang Shen, Robert W. Heath Jr., Jeffrey G. Andrews, and Brian L. Evans

Department of Electrical and Computer Engineering, University of Texas at Austin, Austin, TX 78712, USA

Received 1 September 2005; Revised 14 February 2006; Accepted 13 March 2006

We analyze the ergodic capacity and channel outage probability for a composite MIMO channel model, which includes both fast fading and shadowing effects. The ergodic capacity and exact channel outage probability with space-time water-filling can be evaluated through numerical integrations, which can be further simplified by using approximated empirical eigenvalue and maximal eigenvalue distribution of MIMO fading channels. We also compare the performance of space-time water-filling with spatial water-filling. For MIMO channels with small shadowing effects, spatial water-filling performs very close to space-time water-filling in terms of ergodic capacity. For MIMO channels with large shadowing effects, however, space-time water-filling achieves significantly higher capacity per antenna than spatial water-filling at low to moderate SNR regimes, but with a much higher channel outage probability. We show that the analytical capacity and outage probability results agree very well with those obtained from Monte Carlo simulations.

1. INTRODUCTION

Multiple-input multiple-output (MIMO) communication systems exploit the degrees of freedom introduced by multiple transmit and receive antennas to offer high spectral efficiency. In narrowband channels, when channel state information is available at the transmitter and instantaneous adaptation is possible, the capacity achieving distribution is found by using the well-known water-filling algorithm [1, 2]. With only average power constraints, a two-dimensional water-filling in both the temporal and spatial domains has recently been shown to be optimal [3, 4]. By studying the empirical distribution of the eigenvalues of Gaussian random matrices [1], two-dimensional water-filling for Rayleigh MIMO channels [3, 4] can be transformed into one-dimensional water-filling for a time-varying SISO channel [5]. With the freedom to optimize the transmit power in both time and spatial domains, two-dimensional space-time water-filling disables data transmission when all of the effective channel gains are not high enough to utilize transmit power efficiently, thereby resulting in a larger ergodic capacity when compared to spatial-only water-filling. In [3], a MIMO channel outage probability is defined to quantify how often the transmission is blocked, and upper bounds in Rayleigh fading channels on this outage probability have been developed. Although the ergodic capacity in i.i.d. MIMO Rayleigh fading channels is well understood, the capacity in MIMO Rayleigh fading channels *with shadowing effects* has not been evaluated, and the exact channel outage probability calculation has not been discussed. Furthermore, while [1–4] have studied either spatial or space-time water-filling, the capacity gain of space-time water-filling over spatial water-filling has not been quantified.

In this paper, we perform space-time water-filling for a mixed MIMO channel model that includes both Rayleigh fading and shadowing effects. We show that the ergodic capacity and the exact channel outage probability can both be evaluated through numerical integrations. Hence, the time-consuming Monte Carlo simulations, that is, generating a large number of channel realizations and then performing averaging, can be avoided. We also show that for Rayleigh channels without shadowing, space-time water-filling gains little in capacity over spatial water-filling. For Rayleigh channels with shadowing, space-time water-filling achieves higher spectral efficiency per antenna over spatial water-filling, with a tradeoff of higher channel outage probability. In either case, space-time water-filling actually has lower computational complexity than spatial water-filling.

2. SYSTEM MODEL

A point-to-point MIMO system is shown in Figure 1. Let N_t and N_r denote the number of transmit and receive antennas,

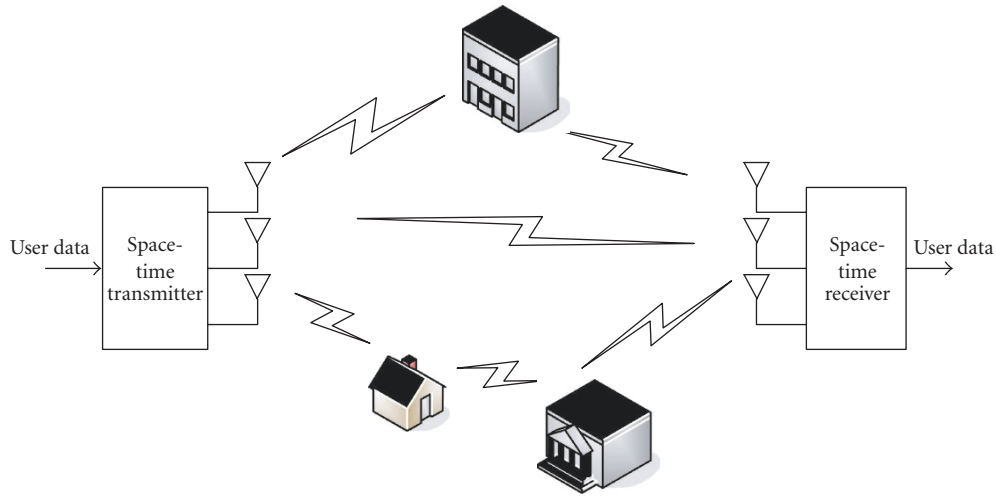

Figure 1: Point-to-point MIMO systems.

respectively. The symbolwise discrete-time input-output relationship of a narrowband point-to-point MIMO system can be simplified as

$$\mathbf{y} = \mathbf{H}\mathbf{x} + \mathbf{v}, \tag{1}$$

where $\mathbf{H}$ is the $N_r \times N_t$ MIMO channel matrix, $\mathbf{x}$ is the $N_t \times 1$ transmitted symbol vector, $\mathbf{y}$ is the $N_r \times 1$ received symbol vector, and $\mathbf{v}$ is the $N_r \times 1$ additive white Gaussian noise vector, with variance $E[\mathbf{v}\mathbf{v}^\dagger] = \sigma^2\mathbf{I}$, where $(\cdot)^\dagger$ denotes the operation of matrix complex conjugate transpose.

In this paper, the MIMO channel $\mathbf{H}$ is modeled as

$$\mathbf{H} = \sqrt{s}\mathbf{H}_w, \tag{2}$$

where $\mathbf{H}_w$ is an $N_r \times N_t$ Rayleigh fast fading MIMO channel whose entries are i.i.d. complex Gaussian random variables [1], and s is a scalar log-normal random variable, that is, $10\log_{10} s \sim \mathcal{N}(0, \rho^2)$, representing the shadowing effect. Notice that log-normal shadowing models the channel *power* variation from objects on large spatial scales; hence, the square root of s is used in (2). Further, shadowing can be modeled as a multiplicative factor to fast fading [6, 7]. Since shadowing occurs on large spatial scales, it is assumed that the shadowing value s equally effects all elements of $\mathbf{H}_w$. Furthermore, s is assumed to be independent of $\mathbf{H}_w$. As the shadowing effect varies slower relative to fast fading, the channel model discussed in this paper is suitable for transmissions over a long time period. Throughout this paper, we assume perfect channel state information is known at the transmitter. The MIMO channel capacity with imperfect channel state information can be found in [8]. Further, we consider MIMO systems with equal numbers of transmit and receive antennas, that is, $N_t = N_r = M$, since expressing the channel eigenvalue distribution is simpler than for unequal numbers of transmit and receive antennas [1]. The same technique discussed in this paper, however, can be applied to MIMO systems with unequal numbers of transmit and receive antennas.

3. SPATIAL AND SPACE-TIME WATER-FILLINGS

3.1. Spatial water-filling

The problem of spatial water-filling for MIMO Rayleigh fading channels was presented in [1]. Channel state information is assumed to be available at the transmitter and power adaption is performed with a total power constraint for each channel realization. The capacity maximization problem can be represented as

$$\max_{\mathbf{Q}} \log\left|\mathbf{I} + \frac{1}{\sigma^2}\mathbf{H}\mathbf{Q}\mathbf{H}^\dagger\right| \quad \text{subject to } \operatorname{tr}(\mathbf{Q}) \le P, \tag{3}$$

where $\mathbf{H}$ is the MIMO channel, $\mathbf{Q}$ is the autocorrelation matrix of the input vector $\mathbf{x}$, defined as $\mathbf{Q} = E[\mathbf{x}\mathbf{x}^\dagger]$, P is the instantaneous power limit, $|\mathbf{A}|$ denotes the determinant of $\mathbf{A}$, and $\operatorname{tr}(\mathbf{A})$ denotes the trace of matrix $\mathbf{A}$.

Notice that $\mathbf{H}^\dagger\mathbf{H}$ can be diagonalized as $\mathbf{H}^\dagger\mathbf{H} = \mathbf{U}^\dagger\Lambda\mathbf{U}$, where $\mathbf{U}$ is a unitary matrix, $\Lambda = \operatorname{diag}\{\lambda_1, \ldots, \lambda_M\}$, and $\lambda_1 \ge \lambda_2 \ge \cdots \ge \lambda_M \ge 0$. It is pointed out in [1] that the optimization in (3) can be carried out over $\widetilde{\mathbf{Q}} = \mathbf{U}\mathbf{Q}\mathbf{U}^\dagger$ and the capacity-achieving $\widetilde{\mathbf{Q}}$ is a diagonal matrix. Let $\widetilde{\mathbf{Q}} = \operatorname{diag}\{q_1, q_2, \ldots, q_M\}$, then the optimal value for q_i is $q_i = (\overline{\Gamma}_0^{(\sigma^2, M)} - \sigma^2/\lambda_i)^+$, where σ^2 is the noise variance, a^+ denotes $\max\{0, a\}$, and $\overline{\Gamma}_0^{(\sigma^2, M)}$ is solved to satisfy $\sum_{i=1}^{M} q_i = P$.

3.2. Space-time water-filling

The problem of two-dimensional space-time water-filling can be formulated as

$$\max_{\mathbf{Q}} E\left[\log\left|\mathbf{I} + \frac{1}{\sigma^2}\mathbf{H}\mathbf{Q}\mathbf{H}^\dagger\right|\right] \quad \text{subject to } E[\operatorname{tr}(\mathbf{Q})] \le \overline{P}, \tag{4}$$

where $\overline{P}$ is the average power constraint; $\mathbf{H}$ and $\mathbf{Q}$ have the same meaning as in (3), that is, $\mathbf{Q} = E[\mathbf{x}\mathbf{x}^\dagger]$ is the covariance

matrix of the transmitted signal for a particular channel realization $\mathbf{H}$. Hence, $\mathbf{Q}$ is a function of $\mathbf{H}$. The expectation in $E[\mathrm{tr}(\mathbf{Q})]$ is carried over all MIMO channel realizations. This notation can be understood as the symbol rate is much faster than the MIMO channel variation and $\mathbf{Q}$ is evaluated from all symbols within one channel realization.

Notice that

$$E\left[\log\left|\mathbf{I}+\frac{1}{\sigma^2}\mathbf{HQH}^{\dagger}\right|\right]=E\left[\sum_{k=1}^{M}\log\left(1+\frac{p(\overline{\lambda}_k)\overline{\lambda}_k}{\sigma^2}\right)\right]$$
$$=ME\left[\log\left(1+\frac{p(\lambda)\lambda}{\sigma^2}\right)\right], \tag{5}$$

where $\overline{\lambda}_k$ is the kth unordered eigenvalue of $\mathbf{H}^{\dagger}\mathbf{H}$, λ denotes any of them, and $p(\lambda)$ denotes the power adaption as a function of λ. Hence, (4) can be rewritten as

$$\max_{p(\lambda)} M\int\log\left(1+\frac{p(\lambda)\lambda}{\sigma^2}\right)f(\lambda)d\lambda$$
$$\text{subject to } M\int p(\lambda)f(\lambda)d\lambda=\overline{P}, \tag{6}$$

where $f(\lambda)$ is the empirical eigenvalue probability density function. The problem in (6) is essentially the same as in [5]. The optimal power adaption is $p(\lambda)=(\Gamma_0^{(\sigma^2,M)}-\sigma^2/\lambda)^+$, where $\Gamma_0^{(\sigma^2,M)}$ is found numerically to satisfy the average power constraint in (6). Notice that the power adaptation is zero for the MIMO channel eigenvalue λ smaller than $\sigma^2/\Gamma_0^{(\sigma^2,M)}$, which means no transmission is allowed in this MIMO eigenmode.

To find $\Gamma_0^{(\sigma^2,M)}$, it is necessary to find $f(\lambda)$ first. From (2), $\mathbf{H}^{\dagger}\mathbf{H}=s\mathbf{H}_w^{\dagger}\mathbf{H}_w$. Let $\{t_k\}_{k=1}^{M}$ be the ordered eigenvalues for $\mathbf{H}_w^{\dagger}\mathbf{H}_w$, that is, $t_1\geq t_2\geq\cdots\geq t_M$. Hence, $\lambda_k=st_k$, where λ_k is the kth largest eigenvalue of $\mathbf{H}^{\dagger}\mathbf{H}$. The ordered joint eigenvalue distribution of Gaussian random matrices $\mathbf{H}_w^{\dagger}\mathbf{H}_w$ has been given in [1, 9] as

$$g_{\text{ordered}}(t_1,t_2,\ldots,t_M)=K_Me^{-\sum_i t_i}\prod_{i<j}(t_i-t_j)^2, \tag{7}$$

where K_M is a normalizing factor.

In this paper, the empirical eigenvalue distribution for $\mathbf{H}_w^{\dagger}\mathbf{H}_w$ is defined to be the probability density function for an eigenvalue t smaller than a certain threshold z. Telatar derived its pdf $g(t)$ by integrating out all other eigenvalues in the unordered joint eigenvalue distribution of Gaussian random matrices [1] to obtain

$$g(t)=\frac{1}{M}\sum_{i=0}^{M-1}L_i^2(t)e^{-t}, \tag{8}$$

where $L_k(t)=(1/k!)e^t(d^k/dt^k)(e^{-t}t^k)$.

Since $10\log_{10}s\sim\mathcal{N}(0,\rho^2)$, by a simple change of variables, the pdf of s can be written as

$$r(s)=\frac{10}{\rho\log 10\sqrt{2\pi}}\frac{1}{s}e^{-(10\log_{10}s)^2/2\rho^2}. \tag{9}$$

Furthermore, s is independent of $\mathbf{H}_w$, hence s is independent of t. The cdf of λ is

$$F(\lambda)=\int_0^{\infty}\int_0^{\lambda/s}r(s)g(t)dt\,ds. \tag{10}$$

Differentiating $F(\lambda)$ with respect to λ generates the pdf of λ:

$$f(\lambda)=\frac{10}{\rho\log 10\sqrt{2\pi}}\int_0^{\infty}g\left(\frac{\lambda}{s}\right)\frac{1}{s^2}e^{-(10\log_{10}s)^2/2\rho^2}ds. \tag{11}$$

With $f(\lambda)$ available, the optimal cutoff value $\Gamma_0^{(\sigma^2,M)}$ can be found by numerically solving

$$M\int_{\sigma^2/\Gamma_0^{(\sigma^2,M)}}^{\infty}\left(\Gamma_0^{(\sigma^2,M)}-\frac{\sigma^2}{\lambda}\right)f(\lambda)d\lambda=\overline{P} \tag{12}$$

and the ergodic capacity can be expressed as

$$E\left[\log\left|\mathbf{I}+\frac{1}{\sigma^2}\mathbf{HQH}^{\dagger}\right|\right]=M\int_{\sigma^2/\Gamma_0^{(\sigma^2,M)}}^{\infty}\log\left(\frac{\Gamma_0^{(\sigma^2,M)}\lambda}{\sigma^2}\right)f(\lambda)d\lambda. \tag{13}$$

4. CHANNEL OUTAGE PROBABILITY

The capacity achieving power distribution from space-time water-filling blocks transmission when all eigenvalues of $\mathbf{H}^{\dagger}\mathbf{H}$ are not high enough to utilize transmit power efficiently. The channel outage probability defined in [3] is equivalent to the probability that the largest eigenvalue of $\mathbf{H}^{\dagger}\mathbf{H}$ is smaller than $\sigma^2/\Gamma_0^{(\sigma^2,M)}$. Since the eigenvalues $\{\lambda_k\}_{k=1}^{M}$ of $\mathbf{H}^{\dagger}\mathbf{H}$ are in descending order, the channel outage probability can be expressed as

$$P_{\text{out}}(\sigma^2,M)=P\left\{\lambda_1\leq\frac{\sigma^2}{\Gamma_0^{(\sigma^2,M)}}\right\}. \tag{14}$$

Although the channel outage probability is defined in [3], only upper bounds in MIMO Rayleigh fading channels on this outage probability are derived. In this paper, the exact channel outage probability is expressed in terms of the maximal eigenvalue distribution, denoted as $f_{\max}(\lambda_1)$.

Recall that $\lambda_1=st_1$, where s is the shadowing random variable and t_1 is the maximal eigenvalue of $\mathbf{H}_w^{\dagger}\mathbf{H}_w$. The

distribution of t_1 is denoted as $g_{\max}(t_1)$ and can be obtained from (7) by integrating out $t_M, t_{M-1}, \ldots, t_2$, that is,

$$g_{\max}(t_1) = \int_0^{t_1} \cdots \int_0^{t_{M-2}} \int_0^{t_{M-1}} K_M e^{-\sum_i t_i} \times \prod_{i<j} (t_i - t_j)^2 dt_M dt_{M-1} \cdots dt_2. \tag{15}$$

Mathematica's built-in function *Integrate* can be used to perform the symbolic integration in (15). For example, when $M = 2$, $g_{\max}(t_1) = e^{-t_1}(2 - 2t_1 + t_1^2 - 2e^{-t_1})$.

With $g_{\max}(t_1)$ available, the same procedure in (9)–(11) can be used to calculate $f_{\max}(\lambda_1)$, with t and $g(t)$ replaced by t_1 and $g_{\max}(t_1)$, respectively. The channel outage probability becomes

$$\begin{aligned} P_{\text{out}}(\sigma^2, M) &= \int_0^{\sigma^2/\Gamma_0^{(\sigma^2,M)}} f_{\max}(\lambda_1)\, d\lambda_1 \\ &= \frac{10}{\rho \log 10 \sqrt{2\pi}} \times \int_0^{\sigma^2/\Gamma_0^{(\sigma^2,M)}} \int_0^{\infty} g_{\max}\left(\frac{\lambda_1}{s}\right) \frac{1}{s^2} e^{-(10\log_{10} s)^2/2\rho^2} ds\, d\lambda_1. \end{aligned} \tag{16}$$

5. APPROXIMATED CAPACITY AND CHANNEL OUTAGE ANALYSIS

Even for medium-sized MIMO systems, for example, $M = 4$ or 6, the calculation of the empirical eigenvalue distribution $g(t)$ in (8) for $\mathbf{H}_w^{\dagger}\mathbf{H}_w$ is computationally intensive, and the resultant $g(t)$ is too complicated to be handled in closed form. Therefore, an approximation to $g(t)$ will be utilized to simplify the calculation of $\Gamma_0^{(\sigma^2,M)}$. An interesting property of Gaussian random matrices is that the distribution of t/M has a limit as the number of antennas increases [1]. Hence,

$$g(t) \approx \frac{1}{2\pi} \sqrt{\frac{4}{tM} - \frac{1}{M^2}}, \quad t \in (0, 4M) \tag{17}$$

as $M \to \infty$. Simulations show that this approximation holds well even for medium-sized MIMO systems, for example, $M = 4$ or 6. With (17), for Rayleigh fading channel with shadowing variance ρ, the cutoff value $\Gamma_0^{(\sigma^2,M)}$ can be found by numerically solving

$$\frac{10M}{(2\pi)^{(3/2)} \rho \log 10} \times \int_{\sigma^2/\Gamma_0^{(\sigma^2,M)}}^{\infty} \int_{\lambda/4M}^{\infty} \left(\Gamma_0^{(\sigma^2,M)} - \frac{\sigma^2}{\lambda}\right) \sqrt{\frac{4s}{\lambda M} - \frac{1}{M^2}} \times \frac{1}{s^2} e^{-(10\log_{10} s)^2/2\rho^2} ds\, d\lambda = \overline{P}. \tag{18}$$

Although the lengthy calculation of $g(t)$ can be avoided with the approximation in (17), the method in (15) to find the maximal eigenvalue distribution $g_{\max}(t_1)$ for channel outage probability analysis still requires a certain amount of computation. In [10], Wong showed that the distribution of the largest singular value of $\mathbf{H}_w$, that is, $\sqrt{t_1}$, can be well approximated with a Nakagami-m distribution. In other words, $g_{\max}(t_1)$ can be approximated with

$$g_{\max}(t_1) = \frac{m^m}{\Gamma(m)\Omega^m} t_1^{m-1} e^{-mt_1/\Omega}, \tag{19}$$

where m and Ω are coefficients dependent on the MIMO system size M; $\Gamma(m)$ is the Gamma function, which is implemented in Mathematica as *Gamma[m]*. Wong also showed the values of m and Ω for different transmit and receive antenna numbers, up to the 6×6 MIMO case [10]. For example, for $M = 4$, $(m, \Omega) = (12.5216, 9.7758)$; for $M = 6$, $(m, \Omega) = (24.0821, 16.5881)$. Substituting (19) into (16), the outage probability can be calculated as

$$P_{\text{out}}(\sigma^2, M) = \frac{10m^m}{\Gamma(m)\Omega^m \rho \log 10 \sqrt{2\pi}} \times \int_0^{\sigma^2/\Gamma_0^{(\sigma^2,M)}} \int_0^{\infty} \left(\frac{\lambda_1}{s}\right)^{m-1} e^{-m\lambda_1/s\Omega} \times \frac{1}{s^2} e^{-(10\log_{10} s)^2/2\rho^2} ds\, d\lambda_1. \tag{20}$$

Table 1: Cutoff value $\Gamma_0^{(\sigma^2,M)}$ for 2×2 MIMO fading channels. The average power constraint is $\overline{P} = 1$. The exact empirical eigenvalue distribution [8] is used in finding $\Gamma_0^{(\sigma^2,M)}$.

SNR	$\rho = 0$		$\rho = 8$		$\rho = 16$	
$(1/\sigma^2)$ (dB)	$\Gamma_0^{(\sigma^2,M)}$	$\overline{P}_{\text{sim}}$	$\Gamma_0^{(\sigma^2,M)}$	$\overline{P}_{\text{sim}}$	$\Gamma_0^{(\sigma^2,M)}$	$\overline{P}_{\text{sim}}$
−5	2.0935	0.9998	1.8233	1.0000	1.5254	1.0181
0	1.2907	0.9998	1.2774	1.0005	1.2098	1.0146
5	0.9075	0.9999	0.9526	0.9999	0.9894	1.0116
10	0.7005	0.9999	0.7576	1.0001	0.8345	1.0098
15	0.5918	0.9999	0.6411	0.9999	0.7255	1.0086
20	0.5392	0.9998	0.5732	1.0000	0.6491	1.0078
25	0.5158	0.9999	0.5356	1.0001	0.5963	1.0071
30	0.5061	0.9999	0.5161	0.9999	0.5606	1.0068

6. NUMERICAL RESULTS AND DISCUSSION

In this section, the achievable spectral efficiencies per antenna of the following three cases are compared by Monte Carlo simulations: (1) space-time water-filling, (2) water-filling in space only, and (3) equal power distribution. We also compare the results from numerical integrations with those obtained from Monte Carlo simulations.

In all simulations, the Rayleigh MIMO channel $\mathbf{H}_w$ has variance of 1/2 for both real and imaginary components. The shadowing effect has a log-normal distribution with standard deviation of ρ [11]. For the pure Rayleigh fading channel, s is a constant of 1. For notational simplicity, we denote the pure Rayleigh fading case as $\rho = 0$. We also study the cases

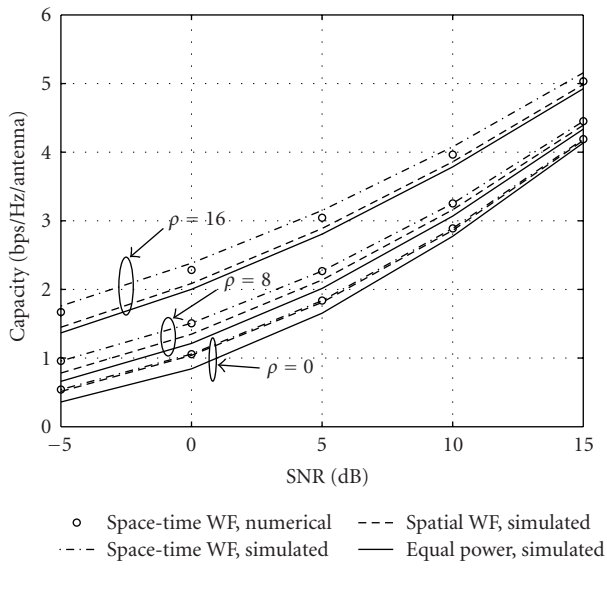

FIGURE 2: Capacity of 2×2 MIMO fading channels. The variance of the log-normal random variable is denoted by ρ. The numerical results are obtained from (13) with Mathematica 5.0.

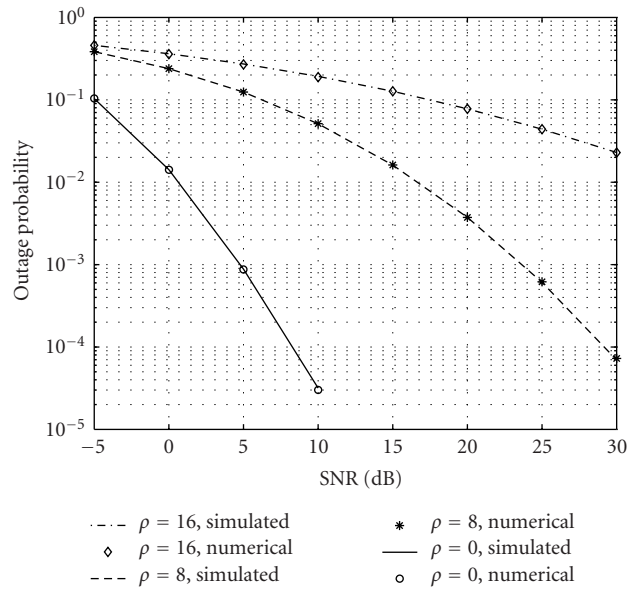

FIGURE 3: Channel outage probability for 2×2 MIMO fading channels. The numerical results are obtained from (16) with Mathematica 5.0. The variance of the log-normal random variable is denoted by ρ.

where $\rho = 8$ and 16. Table 1 shows the cutoff values for a 2×2 MIMO system with different SNRs and log-normal shadowing variances. These cutoff values are obtained from the numerical method *NIntegrate* in Mathematica 5.0. The average power constraint is $\overline{P} = 1$. In Table 1, the columns $\overline{P}_{\text{sim}}$ show the average power obtained in Monte Carlo simulations. If the cutoff value $\Gamma_0^{(\sigma^2, M)}$ is calculated exactly, then $\overline{P}_{\text{sim}}$ will equal $\overline{P}$. Table 1 shows that for $\rho = 0$ and 8, the cutoff values are very accurate. For $\rho = 16$, $\overline{P}_{\text{sim}}$ has 1-2% relative error compared to $\overline{P}$, which is primarily caused by the limited accuracy in the process of numerically finding $\Gamma_0^{(\sigma^2, M)}$ for high shadowing variances.

Figure 2 shows the capacity per antenna versus SNR under different shadowing variances. For Rayleigh channels without shadowing, spatial water-filling achieves almost the same capacity as space-time water-filling. However, for Rayleigh channels with shadowing variance $\rho = 8$, the space-time water-filling algorithm achieves approximately 0.15 bps/Hz/antenna over spatial water-filling at low SNRs, and has a 1.7 dB SNR gain over equal power distribution at a spectral efficiency of 2 bps/Hz/antenna. For Rayleigh fading with shadowing variance $\rho = 16$, space-time water-filling achieves 0.3 bps/Hz/antenna over spatial water-filling. Notice that compared to the pure Rayleigh fading case, the average channel power is increased with the introduction of shadowing, but this does not affect the comparison between 2D and 1D water-fillings. Further, Figure 2 shows that the numerical results evaluated from (13) with Mathematica 5.0 agree with the Monte Carlo results.

Figure 3 shows the channel outage probability for a 2×2 MIMO system. With the increase of the shadowing variance, higher channel outage probability is observed. Figure 3 also presents the channel outages evaluated from (16) with Mathematica 5.0, and the results again agree very well with those obtained from Monte Carlo simulations.

Table 2 shows the cutoff values $\Gamma_0^{(\sigma^2, M)}$ and $\overline{P}_{\text{sim}}$ for 4×4 and 6×6 MIMO systems. The cutoff values are evaluated with the approximation in (17). Even with the approximated empirical eigenvalue distribution, the cutoff values are still very accurate, which is partially shown by the fact that $\overline{P}_{\text{sim}}$ has a relative error not exceeding 2.5% compared to $\overline{P}$.

Figure 4 shows the capacity per antenna for a 4×4 MIMO system. The capacity per antenna for the 6×6 case is very close to the 4×4 case. From Figures 2 and 4, the capacity per antenna is insensitive to the number of antennas in the system. Numerical results from (13) are also shown in Figure 4.

Figure 5 shows the channel outage probability for the 4×4 and 6×6 MIMO systems, with shadowing variance $\rho = 8$. The outage probability is evaluated through (20). For the same shadowing variance, the outage probabilities for the 4×4 and 6×6 MIMO systems are very close, since the shadowing variable equally effects all eigenvalues of $\mathbf{H}_w^{\dagger}\mathbf{H}_w$ and therefore dominates the channel outage probability. Figure 5 shows that even with the approximated maximal eigenvalue distribution, the results from (20) still agree with the Monte Carlo simulations very well.

We also compare the main advantages and disadvantages of space-time water-filling versus spatial water-filling in Table 3. For space-time water-filling, only the cutoff threshold needs to be precomputed, while for spatial water-filling, the optimal power distribution needs to be computed for each channel realization to achieve capacity. On the other hand, the two-dimensional algorithm requires *a priori* knowledge of the channel eigenvalue distribution in order

Table 2: Cutoff value $\Gamma_0^{(\sigma^2,M)}$ for 4×4 and 6×6 MIMO fading channels. The average power constraint is $\overline{P}=1$. The approximated empirical eigenvalue distribution [8] is used in finding $\Gamma_0^{(\sigma^2,M)}$.

SNR	$M=4,\rho=0$		$M=4,\rho=8$		$M=6,\rho=0$		$M=6,\rho=8$	
$(1/\sigma^2)$ (dB)	$\Gamma_0^{(\sigma^2,M)}$	$\overline{P}_{\text{sim}}$	$\Gamma_0^{(\sigma^2,M)}$	$\overline{P}_{\text{sim}}$	$\Gamma_0^{(\sigma^2,M)}$	$\overline{P}_{\text{sim}}$	$\Gamma_0^{(\sigma^2,M)}$	$\overline{P}_{\text{sim}}$
−5	1.0532	1.0010	0.9185	1.0019	0.7021	0.9996	0.6123	1.0015
0	0.6443	0.9988	0.6468	1.0036	0.4295	1.0001	0.4312	1.0016
5	0.4532	1.0050	0.4854	1.0057	0.3021	0.9999	0.3236	1.0023
10	0.3583	0.9994	0.3888	1.0087	0.2389	1.0029	0.2592	1.0038
15	0.3090	1.0070	0.3310	1.0124	0.2060	0.9998	0.2206	1.0053
20	0.2826	1.0204	0.2967	1.0157	0.1884	1.0068	0.1978	1.0082
25	0.2681	1.0243	0.2767	1.0177	0.1787	1.0142	0.1844	1.0101
30	0.2601	1.0208	0.2651	1.0169	0.1734	1.0155	0.1767	1.0111

Table 3: Comparison of space-time and spatial water-fillings.

	Space-time water-filling	Spatial water-filling
Computational complexity	Low	High
Channel eigenvalue distribution	Required	Not required
Ergodic capacity	High	Low
Outage probability	High	Low
Transmission mode	Block transmission	Continuous transmission

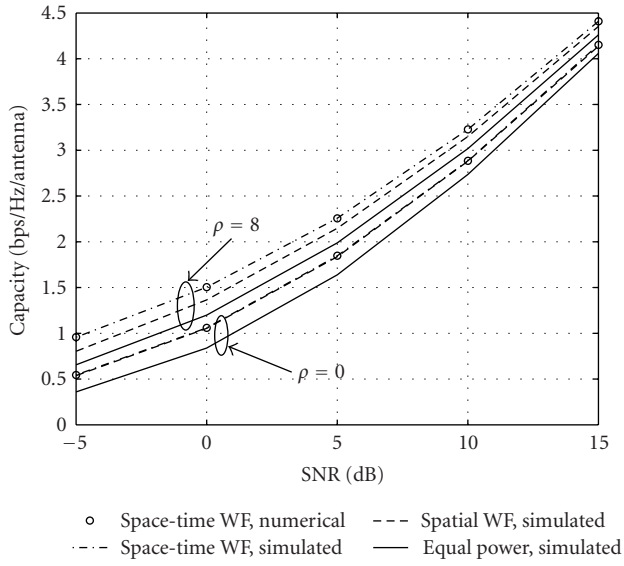

Figure 4: Capacity of 4×4 MIMO fading channels. The variance of the log-normal random variable is denoted by ρ. The numerical results are obtained from (13) with Mathematica 5.0.

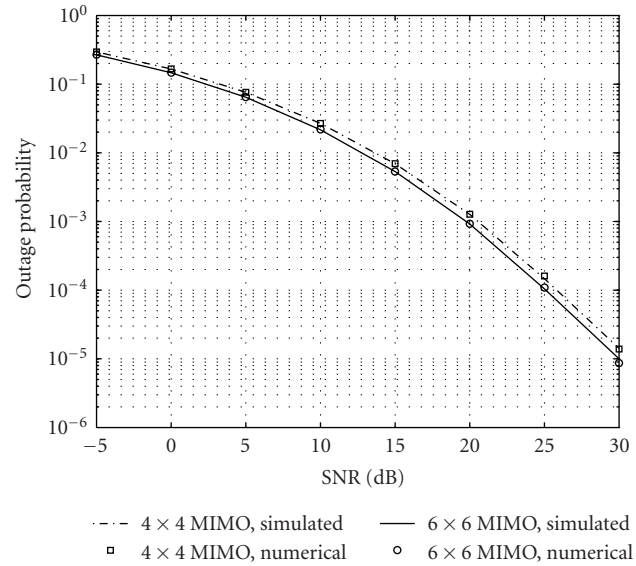

Figure 5: Channel outage probability for 4×4 and 6×6 MIMO fading channels. The numerical results are obtained from (20) with Mathematica 5.0. The variance of the log-normal random variable is $\rho=8$.

to calculate the optimal cutoff threshold. Furthermore, the higher capacity achieved by two-dimensional water-filling comes with a larger channel outage probability. Since shadowing changes much slower than fast fading, the transmission of space-time water-filling is subject to long periods of outage and hence is similar to block transmission. For spatial water-filling, the transmission mode is continuous since for every channel realization, the transmitter always has power to transmit. Further, the capacity gap between space-time and spatial water-filling depends on the distributions of the fast

fading and shadowing gains. An analytical expression for the gap, however, is difficult to obtain.

7. CONCLUSION

In this paper, the ergodic capacity and channel outage probability in a composite MIMO channel model with both fast fading and shadowing have been analyzed. With the eigenvalue distribution of MIMO fading channels, both the capacity and the channel outage probability have been evaluated through numerical integration, which avoids time-consuming Monte Carlo simulations and provides more direct insight into the system. Furthermore, approximations to the empirical eigenvalue distribution and the maximal eigenvalue distribution can greatly simplify the capacity and outage probability analysis. Numerical results illustrate that while the capacity difference is negligible for Rayleigh fading channels, space-time water-filling has an advantage when large-scale fading is taken into account. In all cases, it is simpler to compute the solution for space-time water-filling because it avoids the cutoff value calculation for each channel realization, but it requires knowledge of the channel distribution. The spectral efficiency gain of space-time water-filling over spatial water-filling is also shown to be associated with a higher channel outage probability. Hence, space-time water-filling is more suitable for burst mode transmission when the channel gain distribution has a heavy tail, and spatial water-filling is preferred for continuous transmission when the channel gain distribution is close to Rayleigh or is unknown.

REFERENCES

[1] I. E. Telatar, "Capacity of multi-antenna Gaussian channels," *European Transactions on Telecommunications*, vol. 10, no. 6, pp. 585–595, 1999.

[2] A. Goldsmith, S. A. Jafar, N. Jindal, and S. Vishwanath, "Capacity limits of MIMO channels," *IEEE Journal on Selected Areas in Communications*, vol. 21, no. 5, pp. 684–702, 2003.

[3] S. K. Jayaweera and H. V. Poor, "Capacity of multiple-antenna systems with both receiver and transmitter channel state information," *IEEE Transactions on Information Theory*, vol. 49, no. 10, pp. 2697–2709, 2003.

[4] E. Biglieri, G. Caire, and G. Taricco, "Limiting performance of block-fading channels with multiple antennas," *IEEE Transactions on Information Theory*, vol. 47, no. 4, pp. 1273–1289, 2001.

[5] A. J. Goldsmith and P. P. Varaiya, "Capacity of fading channels with channel side information," *IEEE Transactions on Information Theory*, vol. 43, no. 6, pp. 1986–1992, 1997.

[6] B. M. Hochwald, T. L. Marzetta, and V. Tarokh, "Multiple-antenna channel hardening and its implications for rate feedback and scheduling," *IEEE Transactions on Information Theory*, vol. 50, no. 9, pp. 1893–1909, 2004.

[7] T. S. Rappaport, *Wireless Communications: Principles and Practice*, Prentice Hall PTR, Upper Saddle River, NJ, USA, 2002.

[8] T. Yoo and A. J. Goldsmith, "Capacity and power allocation for fading MIMO channels with channel estimation error," to appear in *IEEE Transactions on Information Theory*.

[9] A. Edelman, *Eigenvalue and condition numbers of random matrices*, Ph.D. thesis, MIT, Cambridge, Mass, USA, May 1989.

[10] K.-K. Wong, "Performance analysis of single and multiuser MIMO diversity channels using Nakagami-*m* distribution," *IEEE Transactions on Wireless Communications*, vol. 3, no. 4, pp. 1043–1047, 2004.

[11] G. L. Stüber, *Principles of Mobile Communication*, Kluwer Academic, Dordrecht, The Netherlands, 2nd edition, 2001.

Zukang Shen received his B.S.E.E. degree from Tsinghua University in 2001, his M.S.E.E. and Ph.D. degrees from The University of Texas at Austin in 2003 and 2006, respectively. He is currently with Texas Instruments, Dallas, Texas. Dr. Shen was awarded the David Bruton Jr. Graduate Fellowship for the 2004–2005 academic year by the Office of Graduate Studies at The University of Texas at Austin. He also received UT Austin Texas Telecommunications Engineering Consortium Fellowships for the 2001–2002 and 2003–2004 academic years. His research interests include multicarrier communication systems, resource allocation in multiuser environments, MIMO channel capacity analysis, digital signal processing, and information theory.

Robert W. Heath Jr. received the B.S. and M.S. degrees from the University of Virginia, Charlottesville, Va, in 1996 and 1997, respectively, and the Ph.D. degree from Stanford University, Stanford, Calif, in 2002, all in electrical engineering. From 1998 to 2001, he was a Senior Engineer then Senior Consultant with Iospan Wireless Inc., San Jose, Calif, where he played a key role in the design and implementation of the physical and link layers of the first commercial MIMO-OFDM communication system. In 2003, he founded MIMO Wireless Inc., consulting company dedicated to the advancement of MIMO technology. Since January 2002, he has been with the Department of Electrical and Computer Engineering at the University of Texas at Austin where he is currently an Assistant Professor and a Member of the Wireless Networking and Communications Group. His research interests include several aspects of MIMO communication such as antenna design, practical receiver architectures, limited feedback techniques, ad hoc networking, scheduling algorithms, and more recently 60 GHz communication. Dr. Heath serves as an Editor for the IEEE Transactions on Communication and an Associate Editor for the IEEE Transactions on Vehicular Technology.

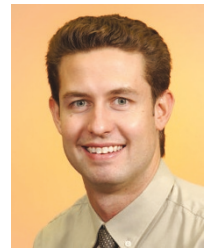

Jeffrey G. Andrews is an Assistant Professor in the Department of Electrical and Computer Engineering at the University of Texas at Austin, and an Associate Director of the Wireless Networking and Communications Group (WNCG). He received the B.S. degree in engineering with high distinction from Harvey Mudd College in 1995, and the M.S. and Ph.D. degrees in electrical engineering from Stanford University in 1999 and 2002, respectively. He developed code-division multiple-access (CDMA) systems as an engineer at Qualcomm from 1995 to 1997, and has served as a frequent consultant on communication systems to numerous corporations, startups, and government agencies, including Microsoft, Palm, Ricoh, ADC, and NASA. Dr. Andrews

serves as an Associate Editor for the IEEE Transactions on Wireless Communications. He also is actively involved in IEEE conferences, serving on the organizing committee of the 2006 Communication Theory Workshop as well as regularly serving as a Member of the technical program committees for ICC and Globecom. He is a coauthor of the forthcoming book from Prentice-Hall, *Understanding WiMAX: Fundamentals of Wireless Broadband Networks*.

Brian L. Evans is the Mitchell Professor of electrical and computer engineering at the University of Texas at Austin in Austin, Texas, USA. His B.S.E.E.C.S. (1987) degree is from the Rose-Hulman Institute of Technology in Terre Haute, Indiana, USA, and his M.S.E.E. (1988) and Ph.D.E.E. (1993) degrees are from the Georgia Institute of Technology in Atlanta, Georgia, USA. From 1993 to 1996, he was a Postdoctoral Researcher at the University of California, Berkeley, in design automation for embedded digital systems. At UT Austin, his research group develops signal quality bounds, optimal algorithms, low-complexity algorithms and real-time embedded software of high-quality image halftoning for desktop printers, smart image acquisition for digital still cameras, high-bitrate equalizers for multicarrier ADSL receivers, and resource allocation for multiuser OFDM basestations. Dr. Evans is the architect of the Signals and Systems Pack for Mathematica. He received a 1997 US National Science Foundation CAREER Award.